Optimization of Venturi Scrubbers Using Genetic Algorithm

G. Ravi,[†] Santosh K. Gupta,[‡] S. Viswanathan,[†] and M. B. Ray*,[†]

Department of Chemical and Environmental Engineering, National University of Singapore, 4 Engineering Drive 4, Singapore 117576, and Department of Chemical Engineering, Indian Institute of Technology, Kanpur 208016, India

Optimization of a venturi scrubber was carried out using a nondominated sorting genetic algorithm (NSGA). Two objective functions, namely, (a) maximization of the overall collection efficiency η_o and (b) minimization of the pressure drop Δp, were used in this study. Three decision variables, the liquid−gas flow ratio L/G, the gas velocity in the throat V_{gth}, and the aspect ratio Z were used. Optimal design curves (nondominated Pareto sets) were obtained for a pilot-scale scrubber. Values of the decision variables corresponding to optimum conditions on the Pareto set were obtained. It was found that the L/G ratio is a key decision variable that determines the uniformity of liquid distribution and the best values of L/G and Z are about 1.0×10^{-3} and 2.5, respectively. In addition, V_{gth} was found to vary from about 40 to 100 m/s as the optimal η_o on the Pareto increased (as did Δp) from about 0.6 to 0.98. The effect of adding a fourth decision variable, the throat length L_o, was also studied. It was found that this leads to slightly lower pressure drops for the same collection efficiency than obtained with three decision variables. An optimum length correlation for the throat of the venturi scrubber was obtained as a function of operating conditions. This study illustrates the applicability of NSGAs in solving multiobjective optimization problems involving gas−solid separations.

Introduction

Venturi scrubbers (Figure 1) have been used extensively throughout the second half of this century as a major gas-cleaning device for the control of fine particulates from industrial exhausts. Their advantages include lower initial costs for comparable collection, low space requirements, the absence of internal moving parts, and the ability to handle wet and corrosive gases. Large power requirements for their operation are the main drawback. Although venturi scrubbers have been designed to operate under optimal conditions, a systematic approach for optimal design is lacking. However, with the use of excellent mathematical models describing the operation of the scrubber in conjunction with modern tools of optimization, one could produce the best possible designs. In this work, the methodology for obtaining the "best" designs for venturi scrubbers, which optimize (maximize or minimize) *several* performance criteria (objective functions) *simultaneously*, using a simple but robust AI-based technique (genetic algorithm, GA) is described.

Models for Efficiency and Pressure Drop Predictions

The success of any optimization process depends on the accuracy of the models used. Several attempts have been made in the past to calculate scrubber efficiency theoretically but with moderate success. The efficiency models of Calvert,[1] Calvert et al.,[2] Boll,[3] Placek and Peters,[4,5] and Cooper and Leith[6] assume complete utilization and uniform distribution of the scrubbing liquid with a varying or average drop size distribution. These one-dimensional models, in general, overpredict the collection efficiency of the particles. This is due to the nonuniform distribution of the liquid and its incomplete utilization because the liquid film on the walls does not participate in the collection process. Azzopardi and Govan[7] accounted for entrainment and the deposition of drops at the wall with reasonable accuracy. Recent models on the collection efficiency of scrubbers have

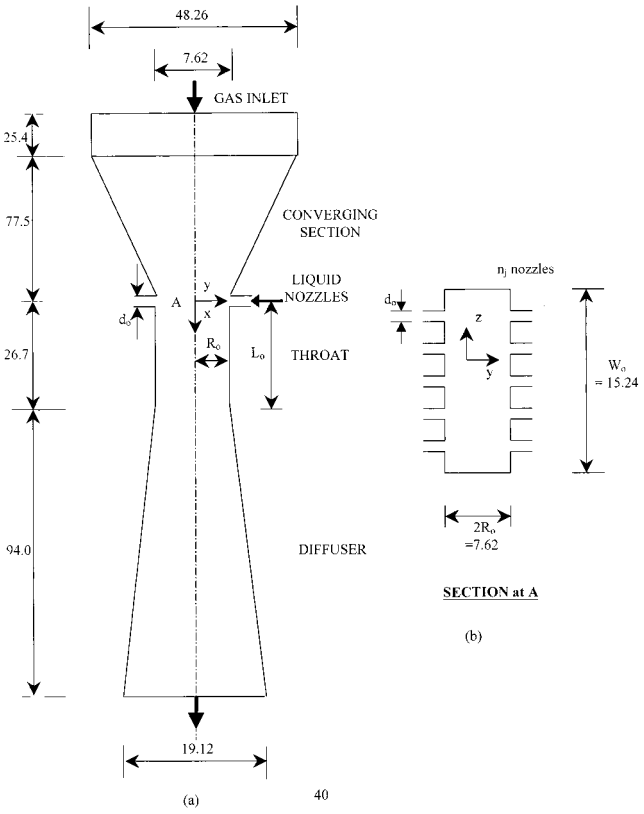

Figure 1. Schematic diagram of a venturi scrubber. Dimensions (cm) as in Ananthanarayanan and Viswanathan.[9]

* To whom correspondence should be addressed. E-mail: cheraym@nus.edu.sg. Fax: (65) 779 1936.
[†] National University of Singapore.
[‡] Indian Institute of Technology.

10.1021/ie010531b CCC: $22.00
Published on Web 05/17/2002

attempted to address the nonuniformity in drop distribution in the throat. Viswanathan[8] proposed a two-dimensional model that is generally adequate for describing the nonuniform flux distribution within the scrubber. Further refinements were made by Ananthanarayanan and Viswanathan[9,10] for the above model with empirical correlations to calculate film flow.

The other important performance characteristic of a venturi scrubber is the pressure drop because it has a direct bearing on the operating cost. Numerous models are available in the open literature for calculating the pressure drop from fundamental mass- and momentum-balance considerations, including the models developed by Calvert,[1] Calvert et al.,[2] Boll,[3] Azzopardi and Govan,[7] Leith et al.,[11] and Allen and van Santen.[12] These models differ in that they use different combinations of gas acceleration, drop acceleration, and frictional effects, with justifications provided. However, all of these models assume a uniform distribution of liquid and do not account for film flow. In addition, other effects such as boundary-layer growth and flow separation in the diffuser are not considered. Hence, these models, though simple, fail to predict the pressure drop accurately over a wide array of operating conditions. Models proposed recently include the annular flow model of Viswanathan et al.[13] and the boundary-layer model of Azzopardi et al.,[14] which endeavor to model film flow effects and diffuser losses, in addition to frictional and acceleration effects. By far, these are the most comprehensive models available for the prediction of pressure drop in venturi scrubbers.

The main performance criteria of venturi scrubbers include the collection efficiency and the associated pressure drop in the scrubber. Although significant progress has been made in developing models for the efficiency and pressure drop, little work has been reported on the optimization of venturi scrubbers. The first study on their optimization was performed by Goel and Hollands,[15] who used the model of Calvert[1] for the determination of the pressure drop and efficiency. They employed a straight-duct approach that does not consider scrubber geometry to estimate the optimum drop diameter. If the liquid is injected upstream of the throat, then the approach requires a multiduct analysis, such as the model of Boll,[3] to determine the optimum throat gas velocity iteratively. They assert that the throat length is insensitive to the overall pressure drop and hence does not affect the optimization results significantly. This is valid if the drops have been accelerated appreciably at the throat entrance, which can happen only if the drops are injected upstream of the throat. However, throat length becomes an important parameter in the optimization of Pease−Anthony-type applications where the liquid is injected in the throat. In addition, charts obtained from numerical search techniques that are specific to drop size prediction methods are required to complete the optimization algorithm. Leith and Cooper[16] proposed an optimization algorithm utilizing the model of Calvert[1] with a straight-duct approach. The Nukiyama−Tanasawa[17] equation was used for estimation of the drop size, and the method employed involved empirical constants that are scrubber-specific. Cooper and Leith[6] presented an improved approach wherein the scrubber geometry was considered and the drag applicable to drops was estimated from the "standard curve" rather than from the Ingebo[18] correlation. This one-dimensional method assumes a uniform coverage of the throat by the drops and so does not consider film flow in the scrubber.

The importance of the nonuniform distribution of droplets was recognized by Haller et al.,[19] when they proposed a two-zone model including droplet-laden and droplet-free zones. They demonstrated experimentally that the occurrence of annular flow within the scrubber system determines the efficiency and the pressure drop. However, their proposed model is too simplistic to determine the flux distribution over a wide range of operating conditions.

The above approaches aim to optimize scrubber performance for two important operating variables, viz., the liquid-to-gas ratio L/G and the gas velocity in the throat V_{gth}. Certain important design parameters, such as the throat dimensions, nozzle diameter, and liquid injection arrangement, that can affect the liquid distribution are not considered. Moreover, these approaches use simplified models that assume a uniform liquid distribution and do not account for film flow. Hence, the above approaches are limited in accuracy and are scrubber-specific. An improved optimization study must take into account both design and operating variables to characterize the nonuniformity of the liquid distribution and the film flow. This requires the use of realistic models for the prediction of pressure drop and collection efficiency. In this work, multiobjective optimization of Pease−Anthony-type scrubbers is carried out using the models developed by Viswanathan[8] for the collection efficiency and Viswanathan et al.[13] for the pressure drop. In this work, an optimization technique is used for the first time in the design of a venturi scrubber.

All of the previous approaches have used conventional simulation techniques to search for the optima. In contrast, a genetic algorithm (GA), a nontraditional search and optimization method introduced by Holland,[20] was used in this work. GA has several advantages over conventional optimization techniques. The advantages of GA over other techniques are as follows: (1) Objective functions can be multimodal or discontinuous. (2) Only information on the objective function is required; gradient evaluation is not required. (3) A starting solution is not needed. (4) The search is carried out using a population of several points simultaneously, rather than a single point, i.e., GA is a population-based approach. (5) GA is better suited to handle problems involving several design or operating variables (called decision variables).

GA mimic the principles of genetics and natural selection, according to the concept of "survival of the fittest", to develop search and optimization procedures. Simple genetic algorithms (SGAs) are suitable for optimization problems involving single-objective functions.[21,22] In such problems, SGAs usually give global optima. In contrast, one might have problems that involve multiple-objective functions, where *unique* optimal solutions might not exist. For example, one might wish to maximize the collection efficiency and, simultaneously, to minimize the pressure drop for a venturi scrubber. In such cases, a *set* of several equally desirable optimal points might exist. These solutions are referred to as Pareto sets or sets of nondominated solutions. No point is superior to any other point in the nondominated set, and indeed, in the absence of additional information, any one of these points could be selected for design or operation. The choice of a *preferred* solution from among the Pareto set of points requires additional knowledge

about the problem, information that can be intuitive and nonquantifiable. Statistical techniques using the opinions of several decision makers are often used to arrive at the preferred solution.[23] However, the Pareto set assists in narrowing down the choices to be considered for a decision maker and, so, is of immense importance. Because GA is a population-based approach, it is ideally suited for finding multiple Pareto-optimal solutions simultaneously. A number of such algorithms are described in a recent text.[24]

A conventional method for solving multiobjective optimization problems is to use a *single* (*scalar*) objective function, which is a weighted average of the several objectives. Unfortunately, the solution obtained in this case depends largely on the values of the weighting factors used, which are not precisely known a priori. Another drawback of the "scalarization" of several objective functions is that some solutions might be missed during the search.[25] In contrast, the nondominated sorting genetic algorithm[24,26] (NSGA) can be used to solve problems involving *vectors* of several objective functions. This technique was first developed by Srinivas and Deb[26] to obtain optimal values of several decision variables associated with the different points of the Pareto set. Subsequently, Mitra et al.[27] extended this technique to solve multiobjective optimization problems wherein the decision variables were continuous *functions*. This enabled the solution of trajectory-optimization problems. The study of Mitra et al.[27] was the first application of NSGAs in chemical engineering. In the past several years, NSGAs have been used to solve a wide variety of complex multiobjective optimization problems of industrial interest in chemical engineering.[27−31] These have been reviewed recently by Bhaskar et al.[32] NSGAs have also been applied[24] to problems outside chemical engineering and, in fact, even beyond science and engineering, e.g., in finance and management.

In this study, an NSGA is used with two objective functions, namely, maximization of the overall collection efficiency and minimization of the pressure drop.

Model for the Collection Efficiency

The performance of a venturi scrubber (see Figure 1) depends largely on the manner of liquid injection, the drop size, the liquid flux distribution, and the initial liquid momenta. The majority of the collection process occurs in the throat because of the presence of a high degree of turbulence in the region caused by the large relative velocities between the drops and particles. Therefore, it is important for the theoretical model to be able to predict the flux distribution within the throat as closely as possible. Ananthanarayanan and Viswanathan[9,10] used a simplified version of the model proposed earlier by Viswanathan.[8] It takes into account the jet penetration length, the nonuniform distribution of liquid drops, the initial momenta of the liquid, and the nonuniformity in the drop size distribution at the inlet. These researchers considered that the movement of the drops is driven by convection in the axial direction (x in Figure 1, the direction of the gas flow) and is due to diffusion in the lateral direction (y in Figure 1, the direction perpendicular to the gas flow). Particulate collection by the droplets is due to inertial impaction of the dust particles onto the droplets. The assumptions of the model include a uniform drop size, a constant film flow, no drop−drop interactions, a uniform inlet distribution of particles, and no interactions between particles. An empirical correlation is used to estimate the fraction of liquid flowing on the walls. The separation distance between the liquid injection orifices is very small. Hence, the variation in the drop concentration can be assumed negligible in the z direction (Figure 1), making the model two-dimensional.[8,13] For reasons of symmetry, only one-half of the scrubber, $0 \le y \le R_o$, is considered for simulation. This simplification reduces the complexity as well as the computational time required for simulation. The equations used for the determination of the collection efficiency for the scrubber shown in Figure 1 are presented in Table 1.[9]

The system chosen is axisymmetric, and hence, the total volume chosen for simulation accounts for one nozzle (in the z direction), the entire length of the scrubber (x direction), and one-half of the width of the scrubber (y direction), as shown in Figure 1. The physical space is divided into cells of a fixed Eulerian grid. The Lagrangian mass particles carry the fluid from cell to cell by the sum of bulk and turbulent velocities. To evaluate the movements of each mass particle, the bulk velocity, eddy diffusivity, gas stream drag, and initial liquid momenta are calculated. The jet penetration length is determined, and subsequently, the flux distribution at any axial position is obtained by applying a central difference formula to the two-dimensional steady-state continuity equation for the liquid drops. Particulate matter is introduced as uniformly distributed dust particles moving with the same velocity as the gas stream. The particle distribution at any axial position is then determined in a way similar to the flux distribution. The overall collection efficiency, η_o, at the end of the scrubber is then determined.

Model for the Pressure Drop

The pressure drop, Δp, in this Pease−Anthony unit is determined using the annular flow model developed by Viswanathan et al.[13] Pressure losses that occur during the acceleration of the gas and of the liquid drops and as a result of frictional losses are predicted. The total pressure drop is calculated after the pressure recovery that occurs in the diffuser is taken into account. The overall collection efficiency and the pressure drop are determined using the equations given in Table 1.

Formulation. The value of the eddy diffusivity, E_p, is critical in the lateral distribution of particles because of diffusion. Values of E_p between 10^{-2} and 10^{-3} m^2/s have been suggested for industrial dusts.[33] A trial-and-error matching of the experimental efficiency was achieved using different values of E_p. This gave rise to the E_p value of 10^{-2} m^2/s that was used in this work.

Several meaningful multiobjective optimization problems can be formulated using the model equations. The methodology used is illustrated with only two objective functions, I_1 and I_2, in this work. The results for such two-objective function problems can be described visually in a very convenient manner using two-dimensional plots of I_2 vs I_1. The two objective functions are (a) maximization of I_1, the overall collection efficiency η_o, and (b) minimization of I_2, the pressure drop Δp.

The decision variables can be identified, and their bounds can be fixed depending on practical considerations. Three decision variables were selected, namely, the liquid-to-gas flow ratio L/G, the gas velocity at the throat V_{gth}, and the aspect ratio Z [$\equiv W_o/(2R_o)$]. The first multiobjective function optimization problem studied

Table 1. Model Equations

Collection Efficiency (Ananthanarayanan and Viswanathan[9])

$$\frac{\partial}{\partial x}(V_{dx}C_d) = \frac{\partial}{\partial y}\left(E_d \frac{\partial C_d}{\partial y}\right) + Q_d - Q_f \quad (4)$$

$$F = \frac{89.379}{\left(\frac{L}{G}\frac{R_o}{d_o}\right)^{1.007}(V_{gth})^{0.888}} \quad (5)$$

$$\frac{dV_{dx}}{dx} = \frac{3}{4}C_{DN}\mu_G\frac{(V_G - V_{dx})}{D_d{}^2\rho_d V_{dx}} \quad (6)$$

$$C_{DN} = C_D N_{Re} \quad (7)$$

$$C_D = \frac{25.8}{N_{Re}{}^{0.81}} \quad (8)$$

$$D_d = \frac{42\,200 + 5776\left(\frac{L}{G}\right)^{1.932}}{V_{gth}{}^{1.602}} \quad (9)$$

$$\frac{E_d}{E_G} = \frac{b^2}{b^2+\omega^2};\quad \frac{E_p}{E_G} = \frac{\omega^2}{b^2+\omega^2} \quad (10)$$

$$0 = -V_G\frac{\partial C_p}{\partial x} + \frac{\partial}{\partial y}\left(E_p\frac{\partial C_p}{\partial y}\right) - \sum_{i=1}^{m^*}\sum_{j=1}^{n^*}\frac{\pi\eta_{ij}F_i}{4}D_{dj}{}^2(V_G - V_{dxj})C_pC_{dj} \quad (11)$$

$$\eta_{ij} = \left(\frac{\psi}{\psi+0.7}\right)^2 \quad (12)$$

$$\eta_o = 1 - \frac{\int C_{p(x,y)}\,dy}{\int C_{p(0,y)}\,dy} \quad (13)$$

$$\frac{l^*}{d_o} = 0.1145\frac{\rho_j V_j}{\rho_G V_{Gth}} \quad (14)$$

Pressure Drop (Viswanathan et al.[13])

$$X = \frac{W_G}{W_c} = \frac{W_G}{W_d + W_G} \quad (15)$$

$$W_f = (1 - C_f)W_L \quad (16)$$

$$W_d = C_f W_L \quad (17)$$

$$W_L = mW_G = W_d + W_f \quad (18)$$

$$\alpha_c = \frac{A_c}{A_T} \quad (19)$$

$$\alpha_G = \frac{Q_{vG}}{Q_{vG} + Q_{vd}} \quad (20)$$

$$A_T\,dP + \frac{W_G\,dV_G}{g_c} + \frac{W_d\,dV_d}{g_c} + \frac{W_f\,dV_f}{g_c} + A_T\,dP_{TP} = 0 \quad (21)$$

$$dP_{TP} = (dP/dz)_c\phi_c{}^2\,dz \quad (22)$$

$$\frac{1}{\rho_c} = \frac{X}{\rho_G} + \frac{(1-X)}{\rho_d} \quad (23)$$

$$\frac{1}{\mu_c} = \frac{X}{\mu_G} + \frac{(1-X)}{\mu_d} \quad (24)$$

$$\left(\frac{dP}{dz}\right)_c = \frac{2}{g_c}\frac{\rho_c}{D_{eq}}\left(\frac{W_c}{A_T\rho_c}\right)2f_c \quad (25)$$

$$\frac{dV_d}{dt} = \frac{3}{4}\frac{\mu_G}{\rho_d}\frac{(V_G - V_d)}{D_d{}^2}C_{DN} \quad (26)$$

$$W_G = \alpha_G A_c V_G \rho_G \quad (27)$$

$$W_d = C_f m\alpha_G A_c V_G \rho_G \quad (28)$$

$$W_f = (1 - C_f)m\alpha_G A_c V_G \rho_G \quad (29)$$

$$\frac{dP}{\rho_G} = \left(\frac{\alpha_G\alpha_c V_G\,dV_G}{g_c}\right) + \left(\frac{C_f m\alpha_G\alpha_c V_G\,dV_d}{g_c}\right) + \left[\frac{(1-C_f)m\alpha_G\alpha_c V_G\,dV_f}{g_c}\right] + \left(\frac{2f_c W_c{}^2\phi_c{}^2\,dZ}{g_c D_{eq}\rho_c A_T{}^2\rho_G}\right) \quad (30)$$

$$\alpha_c = (1 + \chi^{0.8})^{-0.378} \quad (31)$$

$$\chi = \sqrt{\frac{\left(\frac{dP}{dz}\right)_f}{\left(\frac{dP}{dz}\right)_c}} \quad (32)$$

$$\phi_c{}^2 = 1 + 12\,\chi + \chi^2 \quad \forall\ N_{Re,f} < 2000$$

$$\phi_c{}^2 = 1 + 12\,\chi + \chi^2 \quad \forall\ N_{Re,f} > 2000 \quad (33)$$

$$\phi_c{}^2 = \left[\frac{1 + 75(1-\alpha_c)}{\alpha_c{}^{2.5}}\right]\left(\frac{W_G + W_d}{W_G}\right)\left[1 - 2\left(\frac{\alpha_c}{1-\alpha_c}\right)\left(\frac{W_f}{W_G}\right)\left(\frac{\rho_G}{\rho_d}\right)\right]^2 \quad (34)$$

$$V_G = \frac{W_G}{\rho_G\alpha_c\alpha_G A_T} \quad (35)$$

$$V_f = \frac{W_f}{\rho_f(1-\alpha_c)A_T} \quad (36)$$

here (referred to as problem 1) is, thus, described mathematically by

$$\text{Max } I_1(u) \equiv I_1\left(\frac{L}{G}, V_{gth}, Z\right) = \eta_o \quad (a)$$

$$\text{Min } I_2(u) \equiv I_2\left(\frac{L}{G}, V_{gth}, Z\right) = \Delta p \quad (b)$$

subject to (s.t.)

$$u_i{}^l \le u_i \le u_i{}^u \quad i = 1, 2, 3 \quad (c)$$

model equations (Table 1) (d) (1)

In this problem, dust having a log−normal distribution

of sizes [mass median diameter (MMD) = 5.0 μm, σ_g = 1.5] is used in the venturi scrubber. An optimal value for L/G obtained earlier[9] for this problem using one decision variable at a time is 1.2×10^{-3}. Accordingly, the values 0.5×10^{-3} and 2.0×10^{-3} m^3 of liquid/m^3 of air were chosen as the bounds for L/G. Bounds for the gas velocity V_{gth} and the aspect ratio Z were determined based on industrial practice. In this work, the throat gas velocities ranged between 20 and 110 m/s. The value of the aspect ratio, Z, used by Ananthanarayanan and Viswanathan[9] in their comparison with a pilot venturi unit was 2.0. A range of 0.5−2.5 was chosen for the aspect ratio in this study. The bounds used for the three decision variables in this problem are, thus, summarized as

$$0.5 \times 10^{-3} \leq L/G \leq 2.0 \times 10^{-3} \text{ m}^3 \text{ of liquid/m}^3 \text{ of air}$$

$$20 \leq V_{gth} \leq 110 \text{ m/s}$$

$$0.5 \leq Z \leq 2.5 \qquad (2)$$

All other dimensions of the venturi scrubber are the same as assumed by Ananthanarayanan and Viswanathan and are given in Figure 1.

In the present study, only three decision variables are used for optimization. Some of the other decision variables that could be used include the length of the diffuser following the throat and its angle. However, models for the determination of the overall collection efficiency in the presence of a diffuser have not yet been developed. Hence, these decision variables are not considered in this study.

The decision variables that lead to an increase in the overall collection efficiency in a venturi scrubber might produce a simultaneous undesirable increase in the pressure drop. Similarly, decision variables that lead to a minimization of the pressure drop might lead to lower collection efficiencies in the scrubber. Thus, the two objective functions in eq 1 are conflicting in nature and would, most likely, lead to a Pareto set of optimal solutions. Paretos are, indeed, obtained, as borne out by our results presented later.

Although an NSGA can be used directly to handle the maximization−minimization problem described in eq 1, we have converted the maximization of the first objective into a minimization using the common procedure.[22] Max $I_1 \Rightarrow$ Min F_1, where F_1 is referred to as a fitness function. We, thus, have the following equivalent two-objective optimization problem to solve

$$\text{Min } F_1 \equiv \frac{1}{1 + I_1} \qquad \text{(a)}$$

$$\text{Min } F_2 \equiv I_2 \qquad \text{(b)}$$

s.t.

$$\text{all earlier constraints(eq 1c and d)} \qquad \text{(c)} \qquad (3)$$

Additional constraints can also be incorporated in the multiobjective optimization problem. For example, a constraint can be imposed such that the collection efficiency is never below 75%. Similarly, a constraint can be imposed such that the pressure drop never exceeds 5000 Pa. One technique of imposing constraints on the objective functions is to use a (large) penalty function P_e (the value used here, somewhat arbitrarily, is 1×10^5). If one wishes to limit the pressure drop to lie below 5000 Pa, the arbitrarily large number P_e can be added to both the fitness functions F_1 and F_2 in eq 3 for all of the chromosomes violating this requirement. This ensures that such chromosomes become unfit and die out almost instantaneously (referred to as instant killing). It should be mentioned that other techniques do exist that could be used to ensure that the constraints on the objective functions are met. One that is particularly useful,[24] at least for NSGAs, is by modifying the definition of dominance in the NSGA. However, we have used the penalty function approach in this work because it is conceptually simple and has been demonstrated[29,32] to work quite well.

Table 2. Parameters Used

computational parameter	value
maximum number of generations, maxgen	80
population size, N_p	50
probability of crossover, p_c	0.65
probability of mutation, p_m	0.001
random seed	0.87619
spreading parameter, σ	0.015
sharing function, α	2
grid size (h), m	0.001
model parameter[a]	**value**
length of inlet, m	0.254
width of inlet, m	0.482
length of converging section, m	0.775
throat length, m	0.267
diffuser length, m	0.0
diffuser angle, °	0.0
density of liquid, kg/m^3	993.0
density of gas, kg/m^3	1.1843
density of particles, kg/m^3	2500
viscosity of liquid, Pa s	1.0×10^{-3}
viscosity of gas, Pa s	1.8×10^{-5}
peclet number	100
number of nozzles	34
MMD, μm	5
standard deviation of inlet dust, σ_g	1.5
E_p, m^2/s	1.0×10^{-2}

[a] Used for simulation in Ananthanarayanan and Viswanathan.[9]

Results and Discussion

The multiobjective optimization problem described in eqs 1 and 3 (and referred to hereafter as problem 1) was solved on a Cray J916 computer. The CPU time required to obtain one set of Paretos was about 1.2 s. A nondominated sorting genetic algorithm[26] was used to obtain the solutions. The values of several of the computational parameters used, as well as the other variables and parameters describing the venturi scrubber, are given in Table 2. The physical dimensions of the venturi scrubber studied here[9] are given in Figure 1. The computer code has been tested on a few simple two-objective function problems described by Deb,[22] as well as on several more complex multiobjective optimization problems.[27−31]

The results of problem 1 are shown in Figure 2 (filled circles and squares). A plot of η_o vs Δp is shown in Figure 2a. This plot has the characteristics of a Pareto set, wherein an improvement (increase) in η_o is accompanied by a worsening (increase) of Δp. Plots of the three decision variables corresponding to the different points on the Pareto set are shown in Figure 2b−d. It is observed that the gas velocity at the throat, V_{gth}, varies along the points on the Pareto. The values of L/G

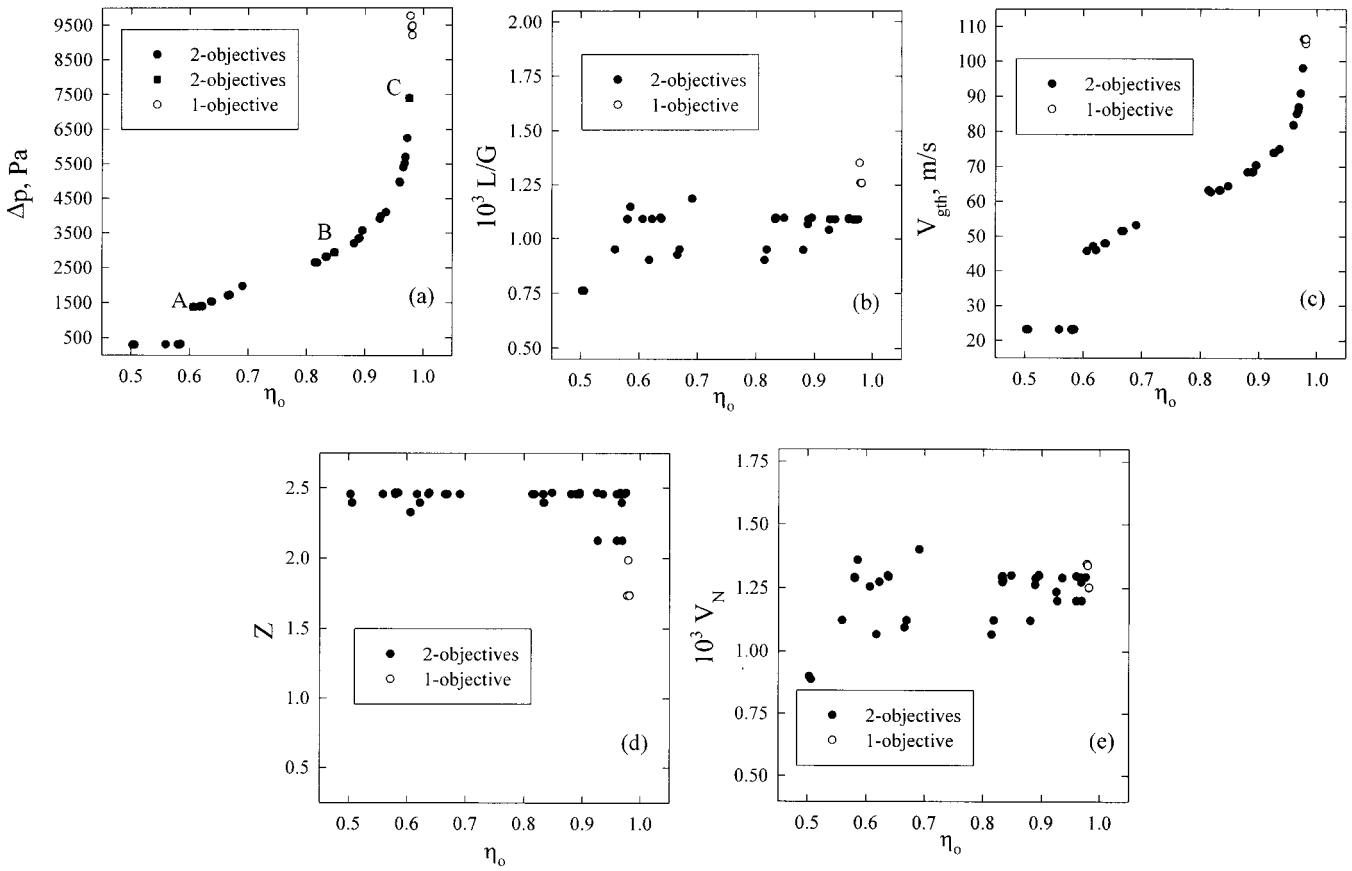

Figure 2. Optimal solutions (filled circles and squares) for the reference case (problem 1, case 1; see Table 3) using three decision variables. Unfilled circles represent the optimal solutions using the NSGA with only a single objective function (maximization of η_o), with E_p constant, and with three decision variables. Δp for the single objective function are computed values. Optimal values of L/G, V_{gth}, Z and V_N for single objective function shown in Figs. 2(b)−(e) are also computed. Filled circles indicate three points, A, B, and C, in the Pareto for case 1 used for detailed study later.

Table 3. Simplified (and Other) Cases Studied for Problems 1 and 2

problem	case	L/G ($\times$ 0^{-3}) (m^3 of liq/m^3 of gas)	V_{gth} (m/s)	Z	objective functions	figure
1	1[a]	0.5−2.0	20.0−110.0	0.5−2.5	η_o, Δp	2
1	2	0.5−2.0	76.2	2.0	η_o, Δp	3
1	3	1.2	20.0−110.0	2.0	η_o, Δp	4
1	4	1.2	76.2	0.5−2.5	η_o, Δp	5
2	1	0.5−2.0	20.0−110.0	0.5−2.5	η_o, Δp	7
2	2	0.5−2.0	76.2	2.0	η_o, Δp	8
2	3	1.2	20.0−110.0	2.0	η_o, Δp	9
2	4	1.2	76.2	0.5−2.5	η_o, Δp	10
1	5	0.5−2.0	20.0−110.0	0.5−2.5	η_o, Δp $\Delta p \leq 4000$ Pa	13
1	6	0.5−2.0	20.0−110.0	0.5−2.5	η_o, Δp $0.25 \leq L_o \leq 0.65$ m	14

[a] Reference case.

that provide optimal operating conditions are found to be almost constant, varying in a narrow range of about $(0.8-1.1) \times 10^{-3}$ (Figure 2b). Similarly, the aspect ratio, Z (Figure 2d), needs to be maintained at around 2.5. Ananthanarayanan and Viswanathan[9] defined a new dimensionless number, called the venturi number V_N [$\equiv LR_oZ/(Gd_on_j)$], that characterizes the nonuniformity in the flux distribution and the overall collection efficiency. They found that this number lies in the range of $(1.0-1.5) \times 10^{-3}$ at the optimal point for an optimization problem involving only one objective function (maximization of the collection efficiency). The computed values of the venturi number for the present problem are shown in Figure 2e. The values of V_N under optimal conditions obtained using NSGA are observed to lie in the same range of $(1.0-1.3) \times 10^{-3}$ earlier found by Ananthanarayanan and Viswanathan.[9]

Three decision variables were used in the multiobjective optimization of venturi scrubbers described in problem 1. These variables interact in a complex manner, creating difficulties in interpreting the optimal solutions. Moreover, the use of several decision variables confers a large degree of freedom to the optimization problem[32] and could lead to numerical problems such as premature convergence[21] and scatter. Considerably more insight is gained by solving (several) simpler multiobjective optimization problems associated with smaller amounts of freedom, such as problems with fewer decision variables. Table 3 summarizes the details of a few such simpler problems. Problem 1, in its most general form (for which Figure 2 applies), involves three decision variables, namely, L/G, V_{gth}, and Z. This is referred to as the reference case (problem 1, case 1). The three simpler versions of this problem are described in

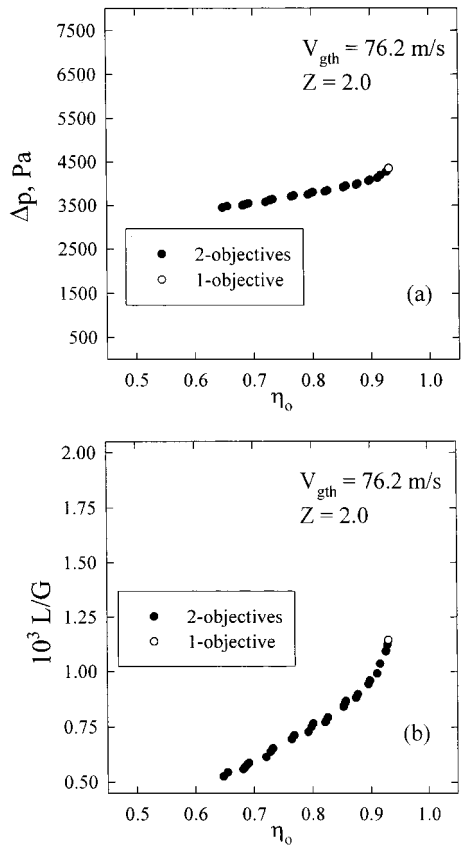

Figure 3. Results for problem 1, case 2, using L/G as the single decision variable. Filled circles use two objective functions, and unfilled circles represent results from the NSGA using a single objective function (maximization of η_o) with E_p constant.

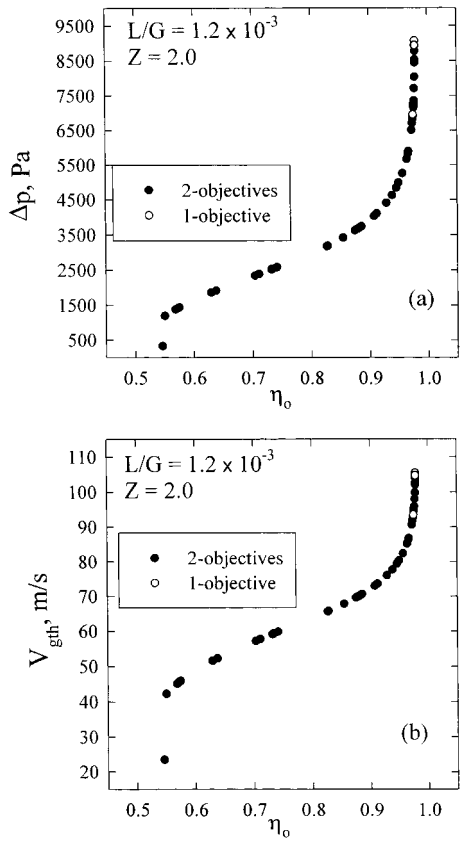

Figure 4. Results for problem 1, case 3, using V_{gth} as the single decision variable. Other details are as in Figure 3.

Table 3 as problem 1, cases 2−4. Each of the latter involves only a single decision variable. The results for these simpler problems are shown in Figures 3−5 (filled circles). It is interesting to observe that the Pareto set obtained with only Z as the decision variable spans a much smaller range of values of η_o and Δp (Figure 5a) than do the Paretos generated using the other decision variables. The sharp increase in Δp with only small changes in η_o in Figure 5a suggests that it is best to use values of Z of about 2.0. A comparison of Figures 3−5 indicates that when only one decision variable is used for optimization, that particular decision variable obviously varies along the Pareto set. In contrast, Figure 2 shows that, when all three decision variables are used simultaneously, only one of them, viz., V_{gth}, varies along the Pareto set, while the other two are somewhat scattered about some mean values, indicating that they are relatively insensitive in determining optimal conditions. On increasing the bounds on Z to $0 \leq Z \leq 2.5$, additional points on the Pareto are obtained, as shown in Figure 5c and d. Clearly, beyond an η_o value of about 0.6, increases in η_o are observed with almost negligible changes in Δp. Of course, very low values of η_o have little use for industrial applications. Figure 5e shows that the Pareto obtained with three decision variables produces lower values of Δp for a given value of η_o than those obtained with any one decision variable, including the one with V_{gth} as the sole decision variable. This phenomenon was found to be true until the efficiency reaches a value of 0.97. The results for case 2 (in Figure 5e) are observed to differ qualitatively from those for the other cases, and significant gains in η_o are achieved with only minimal increases in Δp, until L/G becomes about 1.2×10^{-3}. This demonstrates clearly the importance of L/G in achieving optimal solutions for η_o and Δp. When the L/G ratio is taken at this optimal value of 1.2×10^{-3}, even a relatively minor increase in V_{gth} results in significant gains in η_o with small increases in Δp (Figure 4). An increase in V_{gth} at a constant L/G ratio leads to higher values of η_o at the expense of slightly higher pressure drops, because of the formation of a larger number of smaller droplets.

It is well-known that the flux distribution of the liquid droplets in the throat influences the overall collection efficiency of the particulate solids. The normalized flux ($\equiv M/M_{av}$) distribution of the liquid, introduced as jets through the nozzles (see Figure 1) at the beginning of the throat, is shown as contour plots in Figure 6, for three arbitrarily selected points, A, B, and C (indicated by filled squares) on the Pareto set of Figure 2a. These three points were selected so as to encompass the entire range of the Pareto set, and correspond to values of η_o of 60, 84, and 97% (Δp values of 1372, 2937, and 7394 Pa, respectively). At high values of V_{gth}, the liquid jets emerging normal to the gas flow from the nozzles are atomized close to the walls (low l^*, eq 11, Table 1), and the droplets penetrate all the way to the center because of the intense turbulence. The flux distribution of the liquid droplets in the throat then becomes quite uniform, as shown in Figure 6c. Although the values of the flux are relatively nonuniform at the injection point, a near-uniform coverage of the liquid droplets is obtained at about 75% of the throat length. The increased availability and spread of the water droplets through most of the throat lead to increased collection of dust particles by the droplets and, thus, to higher collection efficiencies. It is important to note that a value of L/G of around 1.2×10^{-3} produces a near-uniform distribution of

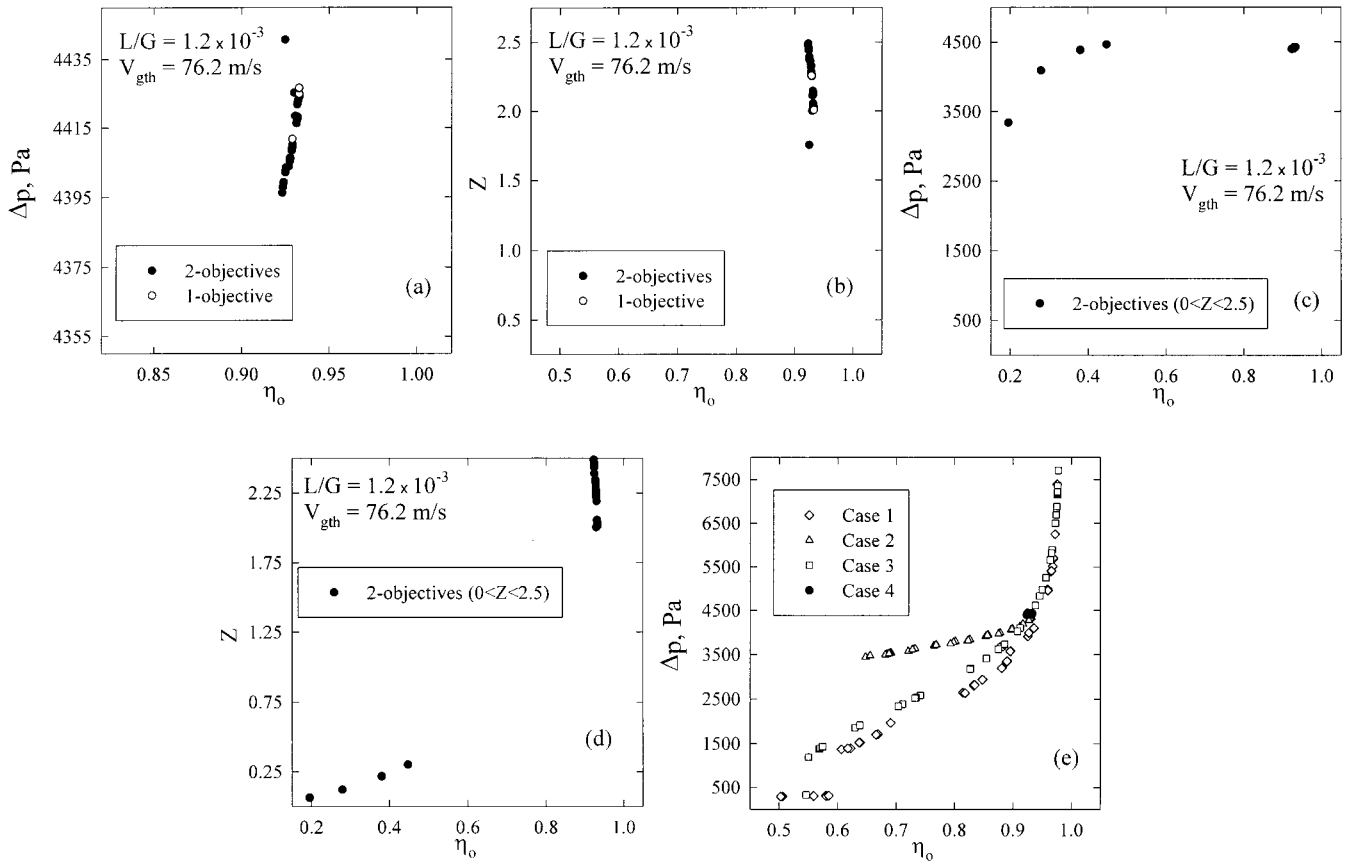

Figure 5. (a, b) Results for problem 1, case 4, using Z as the single decision variable. Other details are as in Figure 3. (c, d) Results for the two-objective function problem with a different bound on Z. (e) Results for all four cases of problem 1.

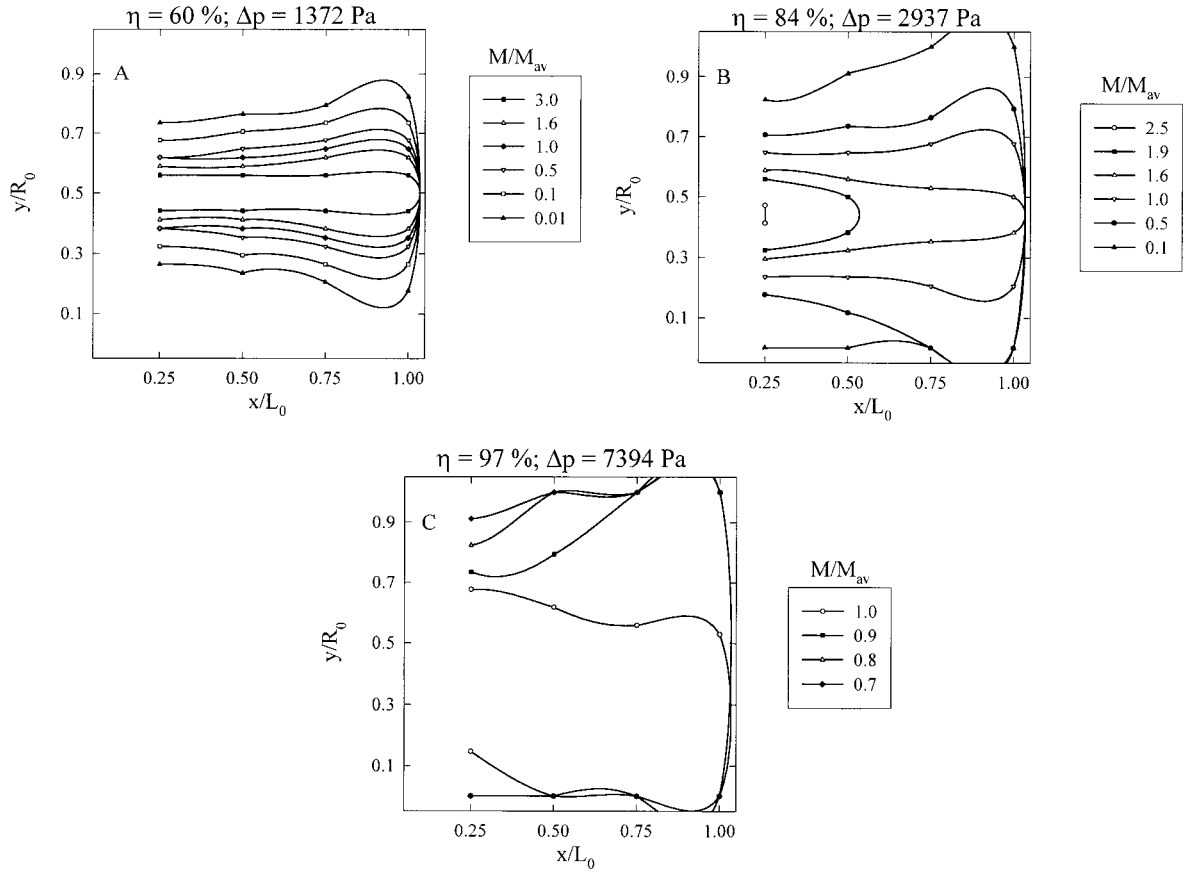

Figure 6. Normalized liquid flux (M/M_{av}) contours in the throat. Plots A, B, and C show the liquid distributions for points A−C in Figure 2a.

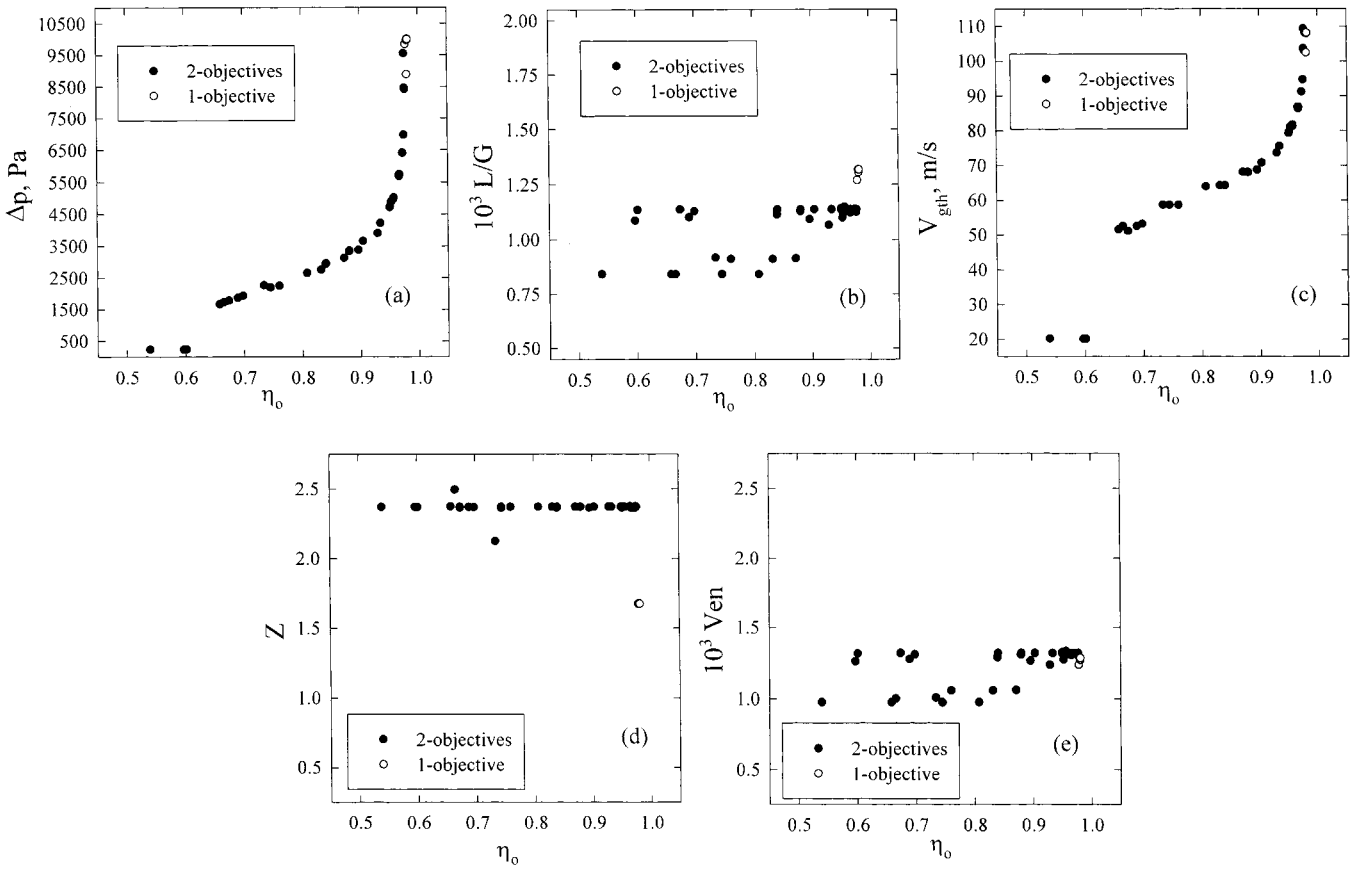

Figure 7. Results for problem 2, case 1, using three decision variables. Filled circles represent results for the two-objective function problem, and unfilled circles represent those from NSGA for a single objective function (maximization of η_o) with E_p constant.

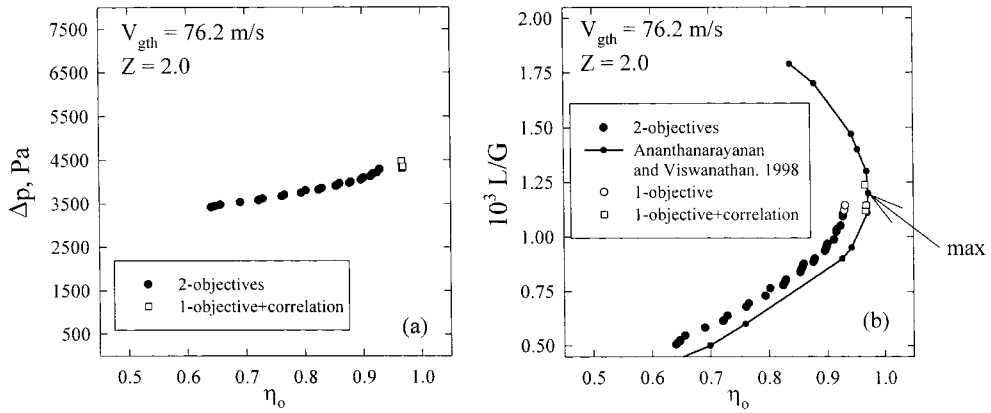

Figure 8. Results for problem 2, case 2, using only the single decision variable L/G. Filled circles represent results for the two-objective-function problem, and unfilled circles represent those from NSGA for a single objective function (maximization of η_o) with E_p constant. Simulation results (computed value of η_o for any L/G) of Ananthanarayanan and Viswanathan[9] are shown by solid curves. Unfilled squares represent optimal solutions from NSGA for a single-objective-function (maximization of η_o) problem, with a correlation used for E_p.

droplets. An increase in V_{gth} at this value of L/G would produce a greater number of finer droplets, and hence, a higher η_o would be obtained. However, increasing V_{gth} beyond a certain value would not be economical because the pressure drop tends to get very high without much return in η_o.

A slightly different multiobjective optimization problem is selected as problem 2. In this problem, all of the solid particles are assumed to have the same size (5 μm). This problem is being studied primarily to compare our optimal solutions using optimization techniques with those obtained by Ananthanarayanan and Viswanathan[9] who used a simulation procedure and considered only the maximization of η_o. The same bounds as in problem 1 (eq 2) for the three decision variables L/G, V_{gth}, and Z are used in this study. The Pareto optimal solutions and the corresponding values of the three decision variables are shown in Figure 7 (filled circles) for problem 2, case 1 (see Table 3). V_{gth}, once again, is found to follow the Pareto as the other two decision variables take on almost constant values (with some scatter), as observed in problem 1. The corresponding simpler problems (problem 2, cases 2−4) involving two objective functions and only a single decision variable are described in Table 3, and the results are shown in Figures 8−10 (filled circles). Figure 10a shows that the optimal Pareto set (for $0.5 \le Z \le 2.5$, as in eq 2) extends over a very narrow range of values of η_o and Δp, somewhat akin to what was observed in Figure 5a. On increasing the bounds of Z to 0 and 2.5, however, several additional

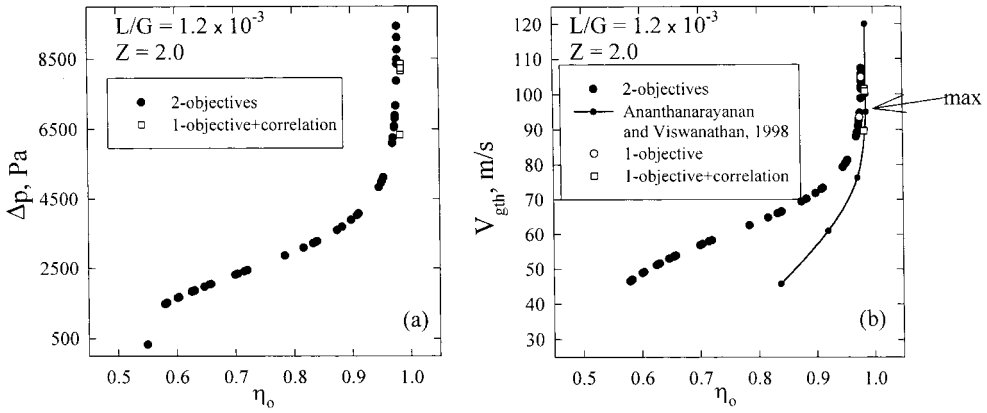

Figure 9. Results for problem 1, case 3, using only the single decision variable V_{gth}. (Notation similar to that in Figure 8.)

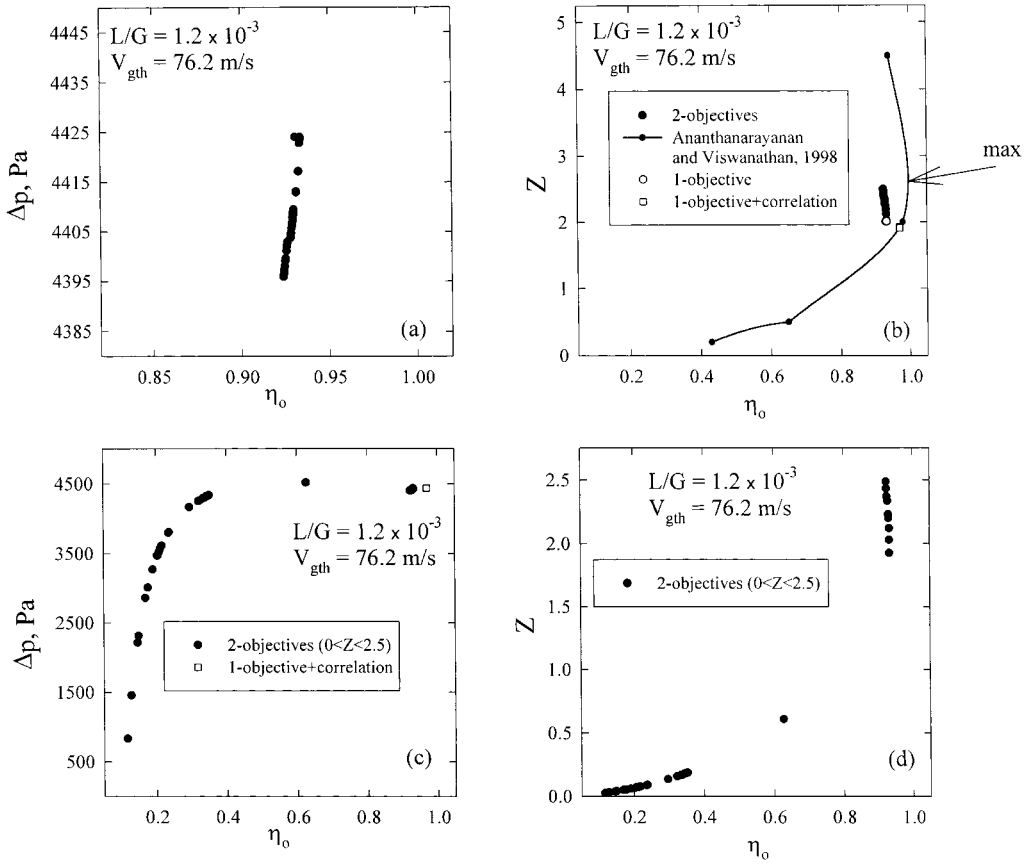

Figure 10. Results for problem 1, case 4, using only the single decision variable *Z*. (Notation similar to that in Figure 8.) Parts c and d show results using extended bounds for *Z*.

points on the Pareto set are obtained, as shown in Figure 10c and d. Figure 10c shows that, beyond η_o values of about 0.6, the Pareto shows almost no variation in Δp with respect to changes in η_o. Hence, lower values of η_o (and, so, of *Z*) are of little practical interest.

The simulation results (calculated values of η_o for selected values of any one variable from among *L*/*G*, V_{gth}, or *Z*) of Ananthanarayanan and Viswanathan[9] are also shown in Figures 8b−10b as curves. These researchers observed a maximum value of the overall collection efficiency η_o in all three cases (indicated by arrows). For example, Figure 8b shows how η_o varies with *L*/*G* (obtained by simulation), and a maximum in η_o is observed at an *L*/*G* value of about 1.2×10^{-3}. Similar maxima in η_o are observed for the other two variables, V_{gth} and *Z*. Because the earlier study[9] considered the effect of one variable at a time to obtain the optimal solution, the solutions obtained through the simulation technique is of limited use. In contrast, the present multiobjective optimization with a single decision variable leads to a Pareto set of several optimal solutions.

The maximization of η_o alone was carried out using the NSGA code. This is similar to the study of Ananthanarayanan and Viswanathan,[9] who used simulations to obtain the optimal point. It should be mentioned that this is the only study on optimization in the open literature with which we can compare at least some of our results. The optimal solutions obtained are shown in Figures 7b−e and 8b−10b as unfilled circles. (Almost) Unique optimal points were obtained, except for some numerical scatter associated with the use of the NSGA. These single-objective-function solutions differ slightly from those obtained by Ananthanarayanan and Viswana-

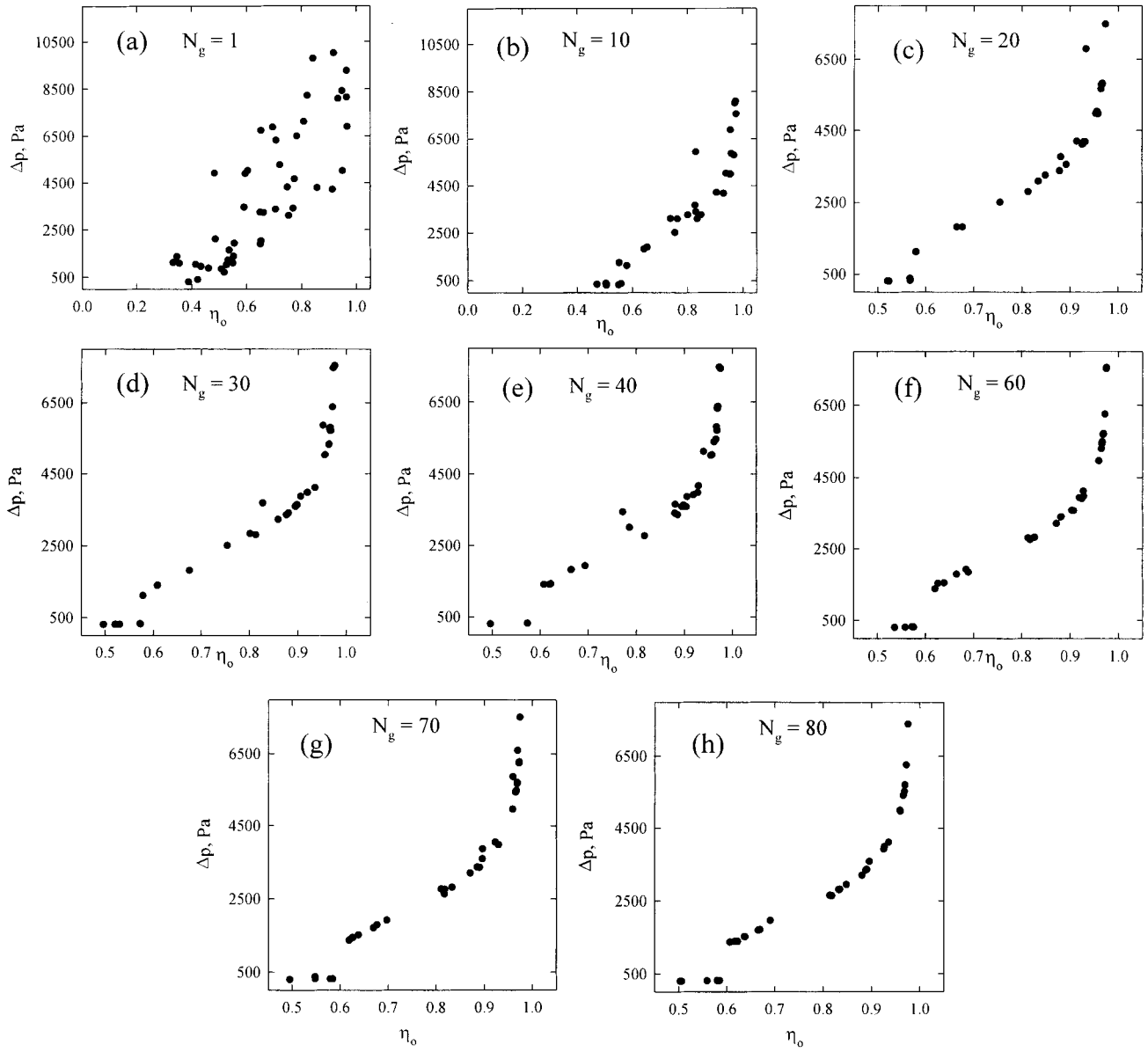

Figure 11. Development of the Pareto set over generations for the reference case (problem 1, case 1).

than,[9] because of the assumption of a constant value of E_p in this study. The earlier study[9] used the correlation $E_p/E_G = \omega^2/b^2 + \omega^2$. The results obtained using the NSGA code with this correlation provided identical solutions, as shown by the unfilled squares in Figures 8b−10b. It is important to note that, for all single-objective optimization results (Figures 7a−9a, 10c), the unfilled circles or squares represent computed values of Δp (corresponding to the optimal values of η_o) and that Δp is not an objective function for these points. It should be mentioned here that the single-objective-function results obtained herein were computed using the NSGA code with both the objective functions identical. The same results were also obtained using the SGA code.[22,24] The use of the NSGA code to study single-objective-function problems, though found appropriate for this problem, need not always be justified because there are some additional computational steps in it that might create numerical problems for single-objective problems at times.

The optimal solutions obtained for problem 1, cases 1−4 (see Table 3), using a single objective function only are shown in Figures 2−5 (unfilled circles, E_p constant). Again, other than some numerical scatter, unique optimal solutions are obtained. It is interesting to observe in Figure 2a that the *computed* value of the pressure drop for the single-objective-function problem is higher than the values on the Pareto set corresponding to two objective functions, and we could possibly select better points (similar η_o but lower Δp) using the Pareto solutions with two objective functions. Also, the venturi number under optimal conditions is about 1.25 $\times 10^{-3}$, even for the problem involving the maximization of η_o with E_p constant.

Effects of Computational Parameters. The effects of computational parameters on the Pareto solutions are described here. Figure 11 shows the distribution of the feasible solutions for different values of the generation number, N_g. An essentially random distribution of feasible solutions is observed in Figure 11a at the first generation ($N_g = 1$). The presence of some feasible solutions having extremely high values of Δp, above about 10 kPa, is to be noted. However, by the end of the 10th generation ($N_g = 10$), these solutions have died

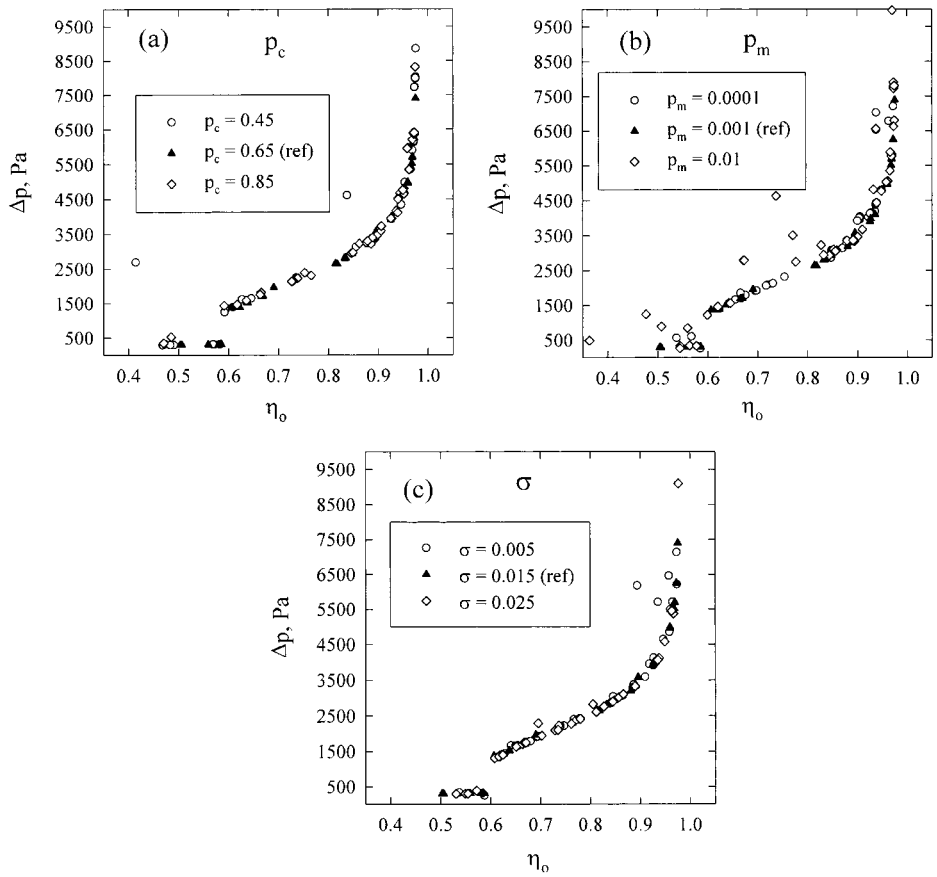

Figure 12. Effects of p_c, p_m, and σ on the Pareto set for the reference case (problem 1, case 1).

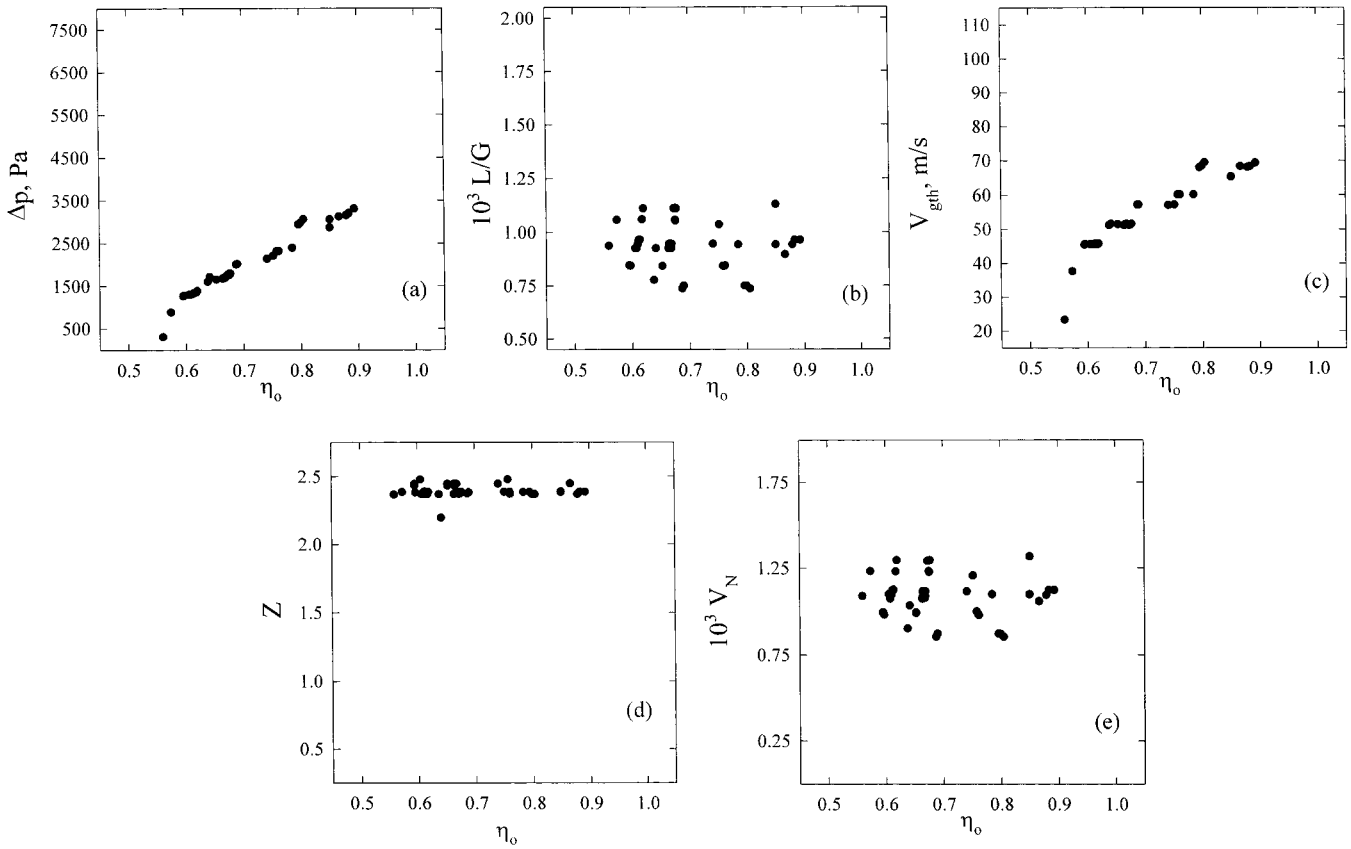

Figure 13. Results for problem 1, case 5.

out, and solutions having lower values of Δp have survived. In addition, a Pareto optimal set seems to have emerged at this stage. Considerable scatter is present, which dies out quite slowly (Figures 11b−f), and by

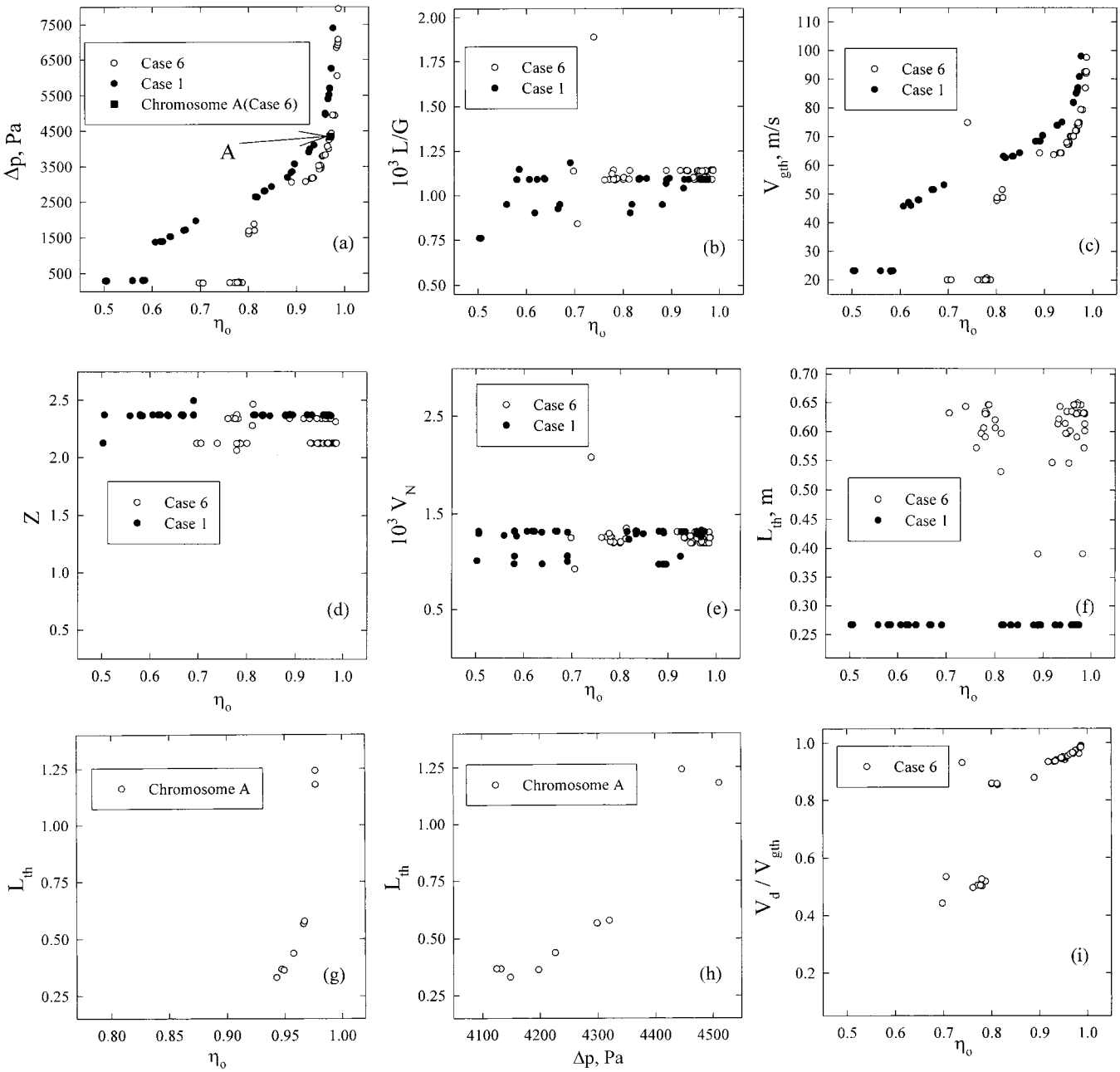

Figure 14. (a−f, i) Optimal solutions for problem 1, case 6. Results for problem 1, case 1, are also shown in parts a−f for comparison. (g, h) Simulation results for chromosome A (filled square in Figure 14a) for different values of the throat length. All other parameters are the same as for chromosome A. (i) V_d/V_{gth} vs η_o for problem 1, case 6.

about the 80th generation, the Pareto seems to have been established. Further generations do not affect the optimal solutions much.

Figure 12 shows the effect of varying the crossover (p_c) and mutation (p_m) probabilities, and the spreading parameter σ on the final Pareto. It is observed that p_c does not have much effect (Figure 12a) on the Pareto optimal curve. However, the same cannot be said for the effect of the mutation probability, p_m. It is observed from Figure 12b that higher values of p_m result in large gaps in the Pareto set as well as some amount of scatter. On the other hand, solutions obtained with lower values of p_m show scatter, particularly at high values of η_o. The best value of this computational parameter is problem-specific and has to be established by trial. The spreading parameter σ determines the range covered by the Pareto set (Figure 12c), and the best value of this parameter also has to be obtained by trial. Unfortunately, the choice of these parameters is problem-specific, and hence, prior knowledge of the appropriate values is unlikely.

Some Additional Optimization Problems. A few more multiobjective optimization problems were also explored. In the first example, an upper bound of 4000 Pa was incorporated on Δp, and the corresponding solutions are shown in Figure 13. It was found that imposition of such a constraint simply truncates the Pareto set of Figure 2, and all points with $\Delta p \geq 4000$ Pa are eliminated. The points obtained differ slightly because of differences in the scatter, and the Paretos and plots of the optimal decision variables in Figures 2 and 13 superimpose quite well.

The multiobjective optimization problem in eq 1 was also solved with four decision variables, with the length of the throat, L_o, being the added variable. This is referred to as problem 1, case 6 (see Table 3). The

bounds of L_o are taken as 0.25 m $\leq L_o \leq$ 0.65 m. The optimal solutions for this case are shown in Figure 14. The solutions for problem 1, case 1, are also shown for comparison. Figure 14a shows that the use of L_o as an additional decision variable leads to higher overall collection efficiencies at a given value of Δp (or a lower Δp for a given η_o) when compared to cases 1−5. Figure 14f shows that the optimal values of L_o are around 0.625−0.65 m, higher than the value of 0.267 m used for all of the previous cases (Figure 1). An optimal value of L_o is, indeed, expected intuitively because, at some operating conditions, the drop velocity, V_d, becomes almost equal to the gas velocity, V_{gth}. Increasing the value of L_o beyond this point would lead to higher values of Δp without any further improvement in the overall collection efficiency. To determine an optimal value of L_o should, indeed, exist, we selected a single chromosome, A, in Figure 14a, and keeping all parameters the same except L_o, we evaluated η_o and Δp for different values of L_o by simulation. The results are shown in Figure 14g and h. Clearly, increasing L_o beyond about 0.6 leads to significant increases in Δp with no improvement in η_o, thus confirming the existence of an optimal value of L_o. Figure 14i shows that the ratio V_d/V_{gth} is close to unity for the Pareto-optimal solutions for case 6 (except for those having very low efficiencies). From the data shown in Figure 14f, an optimum length of the throat can be correlated to operating variables such as L/G and V_{gth} as $L_{opt} = 369.56(LG)^{0.81}/V_{gth}^{0.217}$. This length assumes the maximum efficiency obtainable at a minimum pressure drop for various operating conditions of a venturi scrubber.

Conclusions

Multiobjective optimization of a venturi scrubber was carried out using an NSGA. A few illustrative problems (maximization of the scrubber efficiency, minimization of the pressure drop) were solved, and Pareto optimal sets were obtained. Three decision variables were used in the present study. These include two operating parameters (viz., L/G, V_{gth}) and a geometrical design variable, the aspect ratio Z. It was found that L/G determines the uniformity of the liquid distribution inside the scrubber, and its optimal value lies around 1.0×10^{-3} for the entire set of Pareto points. V_{gth} was found to vary along the Pareto set from about 40 to 100 m/s as the optimum value of η_o on the Pareto increases (as does Δp) from about 0.6 to 0.98. The optimum value of Z is about 2.5 for all of the Pareto points. In addition, it was observed that Pareto solutions having high values of η_o are associated with more uniform distributions of the liquid. Several other interesting multiobjective optimization problems were also studied to enable us to interpret the optimal solutions physically. The Pareto solutions obtained in this work are essentially design curves that assist in narrowing down the choices of a decision maker. Multiobjective optimization problems more complex than those studied here can be solved and interpreted in a similar manner, e.g., studies using more complex, three-dimensional models of the venturi scrubber or more complete models incorporating the effects of diffuser design on the collection efficiency.

Nomenclature

$\vec{a}$ = instantaneous drop acceleration, m/s^2
A = cross-sectional flow area of the scrubber, m^2
$b = 18\mu_G/\rho D^2$
C = concentration, number/m^3
C_D = standard drag coefficient
C_{DN} = modified drag coefficient, $C_{DN} = C_D N_{Re}$
C_f = core entrainment factor
d_o = orifice diameter, mm
D = diameter, m
E = eddy diffusivity, m^2/s
f = friction factor
F = fraction of total injected liquid flowing as film on the scrubber walls
F_i = mass fraction of particulate matter belonging to the ith class
F_1, F_2 = fitness functions
$\vec{g}$ = acceleration due to gravity, m/s^2
g_c = gravitational conversion constant, kg m/(N s^2)
L_o = length of the venturi throat, mm
I_1, I_2 = objective functions
l^* = jet penetration length at which the droplets form, mm
L/G = liquid-to-gas flow ratio (L, G in m^3/s)
m = ratio of mass flow rate of liquid to mass flow rate of gas
m^* = number of selected mean diameters describing the particulate matter size range
M = flux distribution of the liquid
MMD = mass median diameter of log−normal distribution, μm
n^* = number of selected mean diameters describing the liquid drop size range
n_j = number of nozzles
N_g = generation number
N_{Re} = Reynolds number
Q_d = liquid drop source strength, number/(m^3 s)
Q_f = amount of liquid flowing as film on the wall, number/(m^3 s)
Q_{vG} = volumetric flow rate of gas, m^3/s
Q_v = volumetric flow rate of drops, m^3/s
p_c = probability of crossover
p_m = probability of mutation
P_e = penalty function
R_o = half-width of venturi throat parallel to water injection, mm
t = time, s
u = decision variable
V = velocity, m/s
V_{gth} = gas velocity at the throat, m/s
V_N = venturi number
W = mass flow rate, kg/s
W_o = width of venturi throat perpendicular to water injection, mm
x, y, z = rectangular coordinates, m
X = core quality
Z = aspect ratio [$\equiv W_o/(2R_o)$]

Greek Symbols

α = exponent controlling the sharing function
α_c = fractional area occupied by homogeneous core
α_G = volume fraction of core occupied by gas
χ = Martinelli parameter
Δp = pressure drop, Pa
η = fractional collection efficiency
η_{ij} = collection efficiency of particulate matter belonging to the ith class by droplets belonging to jth class
η_o = overall collection efficiency
μ = fluid viscosity, kg/(m s)
ρ = density, kg/m^3
σ = spreading parameter
σ_g = standard deviation of log−normal distribution
φ^2 = two-phase friction multiplier
ψ = impaction parameter, $|V_G - V_{dN}|P_\rho D_\rho^2/9\mu_G D_d$
ω = frequency of air fluctuations, rad/s

Subscripts

av = average
c = core
d = drop
eq = equivalent
f = film
g, G = gas
i = index of decision variable
j, L = jet or liquid
max = maximum
ov = overall
p = particle/dust
th = throat
T = total
TP = two-phase
x, *y*, *z* = rectangular coordinates

Superscripts

l = lower limit
u = upper limit

Literature Cited

(1) Calvert, S. Venturi and Other Atomizing Scrubbers. *AIChE J*. **1970**, *16*, 392.

(2) Calvert, S.; Lundgren, D.; Mehta, D. S. Venturi Scrubber Performance. *J. Air Pollut. Control Assoc.* **1972**, *22*, 529.

(3) Boll, R. H. Particle Collection and Pressure Drop in Venturi Scrubbers. *Ind. Eng. Chem. Fundam*. **1973**, *12*, 40.

(4) Placek, T. D.; Peters, L. K. Analysis of Particulate Removal in Venturi Scrubbers—Effect of Operating Variables on Performance. *AIChE J*. **1981**, *27*, 984.

(5) Placek, T. D.; L. K. Peters. Analysis of Particulate Removal in Venturi Scrubbers—Role of Heat and Mass Transfer. *AIChE J*. **1982**, *28*, 31.

(6) Cooper, D. W.; Leith, D. Venturi Scrubber Optimization Revisited. *Aerosol Sci. Technol*. **1984**, *3*, 63.

(7) Azzopardi, B. J.; Govan, A. H. The Modelling of Venturi Scrubbers. *Filtr. Sep.* **1984**, *23*, 196.

(8) Viswanathan, S. Modeling of Venturi Scrubber Performance. *Ind. Eng. Chem. Res*. **1997**, *36*, 4308.

(9) Ananthanarayanan, N. V.; Viswanathan, S. Estimating Maximum Removal Efficiency in Venturi Scrubbers. *AIChE J*. **1998**, *44*, 2549.

(10) Ananthanarayanan, N. V.; Viswanathan, S. Predicting Liquid Flux Distribution and Collection Efficiency in Cylindrical Venturi Scrubbers. *Ind. Eng. Chem. Res*. **1999**, *38*, 223.

(11) Leith, D.; Cooper, D. W.; Rudnick, S. Venturi Scrubbers: Pressure Loss and Regain. *Aerosol Sci. Technol.* **1985**, *4*, 239.

(12) Allen, R. W. K.; van Santen, A. Designing for Pressure Drop in Venturi Scrubbers: The Importance of Dry Pressure Drop. *Chem. Eng. J*. **1996**, *61*, 203.

(13) Viswanathan, S.; Gnyp, A. W.; St. Pierre, C. C. Annular Flow Pressure Drop Model for Pease−Anthony-Type Venturi Scrubbers. *AIChE J*. **1985**, *31*, 1947.

(14) Azzopardi, B. J.; Teixeira, S. F. C. F.; Govan, A. H.; Bott, T. R. An Improved Model for Pressure Drop in Venturi Scrubbers. *Trans. Inst. Chem. Eng.* **1991**, *69* (B), 237.

(15) Goel, K. C.; Hollands, K. G. T. Optimum Design of Venturi Scrubbers. *Atmos. Environ*. **1977**, *11*, 837.

(16) Leith, D.; Cooper, D. W. Venturi Scrubber Optimization. *Atmos. Environ*. **1980**, *14*, 657.

(17) Nukiyama, S.; Y. Tanasawa, Experiments on Atomization of Liquids in an Air Stream. *Trans. Soc. Mech. Eng., Tokyo* **1938**, *4*, 86.

(18) Ingebo, R. D. Drag Coefficients for Droplets and Solid Spheres in Clouds Accelerating in Air Streams. *NACA Technol. Note* **1956**, 3762.

(19) Haller, H.; Muschelknautz, E.; Schultz, T. Venturi Scrubber Calculation and Optimization. *Chem. Eng. Technol*. **1989**, *12*, 188.

(20) Holland, J. H. *Adaptation in Natural and Artificial Systems*; University of Michigan Press: Ann Arbor, MI, 1975.

(21) Goldberg, D. E. *Genetic Algorithms in Search, Optimization, and Machine Learning*; Addison-Wesley: Reading, MA, 1989.

(22) Deb, K. *Optimization for Engineering Design: Algorithms and Examples*; Prentice Hall of India: New Delhi, India, 1995.

(23) Chankong, V.; Haimes. Y. Y. *Multiobjective Decision Making—Theory and Methodology*; Elsevier: New York, 1983.

(24) Deb, K. *Multi-objective Optimization Using Evolutionary Algorithms*; Wiley: Chichester, U.K., 2001.

(25) Goicoechea, A.; Hansen, D. R.; Duckstein, L. *Multiobjective Decision Analysis with Engineering and Business Applications*; Wiley: New York, 1982.

(26) Srinivas, N.; Deb, K. Multiobjective Function Optimization Using Nondominated Sorting Genetic Algorithms. *Evol. Comp*. **1995**, *2*, 221.

(27) Mitra, K.; Deb, K.; Gupta, S. K. Multiobjective Dynamic Optimization of an Industrial Nylon 6 Semibatch Reactor Using Genetic Algorithm. *J. Appl. Polym. Sci.* **1998**, *69*, 69.

(28) Garg, S.; Gupta, S. K. Multiobjective Optimization of a Free Radical Bulk Polymerization Reactor Using Genetic Algorithm. *Macromol. Theory Simul.* **1999**, *8*, 46.

(29) Bhaskar, V.; Gupta, S. K.; Ray, A. K. Multiobjective Optimization of an Industrial Wiped Film Poly(ethylene terephthalate) Reactor. *AIChE J*. **2000**, *46*, 1046.

(30) Chan, C. Y.; Aatmeeyata; Gupta, S. K.; Ray, A. K. Multiobjective Optimization of Membrane Separation Modules Using Genetic Algorithm. *J. Membrane Sci.* **2000**, *176*, 177.

(31) Rajesh, J. K.; Gupta, S. K.; Rangaiah, G. P.; Ray, A. K. Multiobjective Optimization of Steam Reformer Performance Using Genetic Algorithm. *Ind. Eng. Chem. Res.* **2000**, *39*, 706.

(32) Bhaskar, V.; Gupta, S. K.; Ray, A. K. Applications of Multiobjective Optimization in Chemical Engineering. *Rev. Chem. Eng.* **2000**, *16*, 1.

(33) Mothes, H.; Löffler, F. Prediction of Particle Removal in Cyclone Separators. *Int. Chem. Eng*. **1988**, *28*, 231.

Received for review June 20, 2001
Revised manuscript received December 17, 2001
Accepted March 27, 2002

IE010531B